# Heat and Mass Transfer Effects on Unsteady MHD Fluid Embedded in Inclined Darcy-Forcheimmer Porous Media with Viscous Dissipation and Chemical reaction


**Abstract**

The Darcy-Forcheimmer in fluid-saturated porous media finds application in a variety of engineering processes such as heat exchanger devices, chemical catalytic reactors and metallurgical applications-hot rolling of wires, drawing of metals and plastic extrusion. Also, entrepreneurial development helps in developing MHD power generation systems. The study therefore, investigated unsteady nonlinear MHD fluid embedded in an inclined Darcy-forchemmer in an inclined porous media.

The governing partial differential equations of the model are reduced to a system of coupled nonlinear ordinary differential equations by applying similarity variables and solved numerically using shooting with fourth-order Runge-Kutta method. The local similarity solutions for different values of the physical parameters were presented for velocity, temperature and concentration. The results for Skin friction, Nusselt and Sherwood numbers were presented and discussed.

The study included MHD fluid mechanisms in this presentation to justify advance in scientific research and the need for computational analysis and applications. The study reported the effects of unsteady MHD fluid flow in Darcy-Forcheimmer in porous media and its implication as gateway to entrepreneurial development and National growth.



**Keywords**: Magnetohydrodynamics, Dissipation, Chemical Reaction, Darcy-Forcheimmer, Entrepreneurial Development


## INTRODUCTION

Heat and mass transfer effects of Magnetohydrodynamics (MHD) fluid embedded over inclined Darcy-Forcheimmer porous media with viscous dissipation and chemical reaction is of great concern in physical sciences, life sciences including entrepreneurial development research that support national development. MHD fluid flow through porous media has wide spread applications in engineering industries and enterpreneurial development. Researchers have worked on combination of heat and mass transfer effects using various parameters but unsteady MHD fluid influence on heat and mass transfer through Darcy–Forcheimmer porous medium is necessary as a result of its applications and effects over time and space.

The study of MHD flow over inclined plate with convective surface boundary conditions with dissipation and chemical reactions has attracted interest of the scholars. The reactions for the interest was born out of its significance in many industrial and manufacturing processes. In view of this, Abraham and Sparrow (2005) investigated friction Drag resulting from the simultaneously imposed motion of a free stream and its bounding surface. The authors developed for determining the streamwise variation of the temperature of a moving sheet in the presence of a co-flowing fluid. Also, Sparrow and Abraham (2005) reported universal solutions for the Streamwise variation of the temperature of a moving sheet in the presence of a moving fluid. Radiative MHD flow over a vertical plate with convective boundary conditions was investigated (Etwire and Seini, 2014). MHD boundary layer flow of heat and mass transfer over a vertical plate in a porous medium with suction and viscous dissipation was presented (Lakshmi, Reddy and Poornima 2012).

In recent time the following works relevant to this research were included, for example Dash, Tripathy, Rashidi, and Mishra (2016) used numerical approach to boundary layer stagnation-point flow past a stretching/shrinking sheet. Bhukta, Dash, Mishra, and Baag, S. (2017) related dissipation effect on MHD mixed convective flow over a stretching sheet through porous medium with non-uniform heat source/sink. Baag, Mishra, Nayak and Acharya (2017) studied the effect of radiation on MHD free convective flow over a stretching sheet in the presence of heat source / sink. In the same manner, Mishra and Bhatti (2017) investigated the simultaneous effects of Chemical reaction and Ohmic heating with heat and mass transfer over a stretching surface using numerical approach. Baag,

Mishra, Hoque and Anika (2018) investigated MHD boundary layer flow over an exponentially stretching sheet past a porous medium with uniform heat source. From those studies the following emanated:

- Transport of momentum and thermal energy in fluid saturated porous media with low porosities are commonly described as Darcy's model for conservation of momentum and by the energy equation based on the velocity field found from this model
- Viscous mechanical dissipation effects are important in geophysical flows and also in certain industrial operations and are usually characterized by the Eckert number.
- In some industrial applications such as fixed-bed catalytic reactor, packed bed heat exchangers and drying, the value of the porosity is maximum at the wall and minimum away from the wall so the porosity of the porous media should be taken as non-uniform. Porosity measurements should be noted not to be constant but varies from the wall to the interior of porous media due to which permeability als varies. Variation of porosity and permeability had greater influence on velocity distribution and on heat transfer.
  Chemical reactions can either be homogeneous or heterogeneous processes. This is a function of whether they occur at an interface or as a single-phase volume reaction. In many chemical engineering processes, there occur the chemical reaction between a foreign mass and fluid in which the plate is moving.

The importance of heat and mass transfer in generating wealth for national development is very pertinent and valuable now the research concentrates on enterpreneural development. These areas where enterpreneural activities are found include: transportation where this addresses engine cooling, automobile radiators, climate control, mobile food storage and so on. In healthcare and biomedical applications, we explore blood warmers, organ and tissue storage, hypothermia and so on. In comfort heating, ventilation and air-conditioning this centres on: air conditioners, water heaters, furnaces, chillers, refrigerators and so on. In the weather and environmental changes we think of making the environment conducive. In a renewable energy system: Flat plate collectors, thermal energy storage, photovoltaic (PV) module cooling, and so on are pertinent.

The mass transfer benefits are: humidification of air in a cooling tower, evaporation of petrol in carburetor of a petrol engine, evaporation of liquid ammonia in the atmosphere of hydrogen in electrolytic refrigerator, dispersion of oxides of sulphur (pollutants) from a power plant discharge of neutron in a nuclear reactor, estimation of depth to which carbon will penetrate in a mild steel specimen during the act of carburising Kumar (2013). Kala, Singh and Kumar (2014) investigated MHD free convective flow and heat transfer over non-linearly stretching sheet embedded in Darcy-forcheimmer porous medium. Amoo and Babayo (2017), Amoo, Babayo and Amoo (2017) had extensively evaluated MHD boundary layer flow of Darcy-forcheimmer in porous media. Thumma and Mishra (2018) Effect of viscous dissipation and Joule heating on MHD Jeffery nanofluid flow with and without multi-slip boundary conditions. In view of the above, this study therefore, sought to compute numerically heat and mass transfer effects of the unsteady MHD fluid flow in inclined Darcy-Forcheimmer porous media with viscous dissipation and chemical reactions.

## FORMULATION OF THE PROBLEM

In this research, consider a free convective, boundary layer flow, heat and mass transfer of viscous incompressible fluid considering exponentially-stretching surface. The flow direction emerging out of a slit at origin and moving with non-uniform velocity in the presence of thermal radiation. The free convective thermal radiation effect on heat and mass transfer of two dimensional fluid flow of a unsteady and incompressible fluid flow over inclined exponentially-stretching sheet under the action of thermal and solutal buoyancy forces. The flow was assumed to be in the x-direction with y-axis normal to it. The geometry and equations governing the

fluid flow of heat and mass transfer is assumed as:

Fs

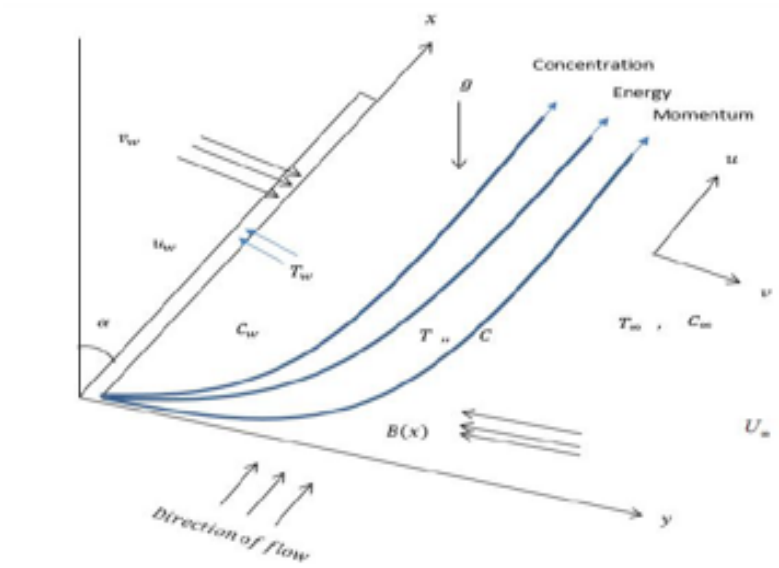


Figure 1: The Geometrical Model and Coordinate system

$$\frac{\partial u}{\partial x}+\frac{\partial v}{\partial y}=0 \tag{1}$$

$$\frac{\partial u}{\partial t}+u\frac{\partial u}{\partial x}+v\frac{\partial u}{\partial y}=-\frac{1}{\rho}\sigma {B_0}^2(x)u+\nu\frac{\partial^2 u}{\partial y^2}-\frac{\mu}{K}u-\frac{b}{\sqrt{K}}u^2+g\beta_T\left(T-T_\infty\right)\cos(\alpha)+g\beta_C\left(C-C_\infty\right)\cos(\alpha)$$

(2)

$$\rho C_p\left(\frac{\partial T}{\partial t}+u\frac{\partial T}{\partial x}+v\frac{\partial T}{\partial y}\right)=k\frac{\partial^2 T}{\partial y^2}-\frac{\partial q_r}{\partial y}+Q_0\left(T-T_\infty\right)+\mu\left(\frac{\partial u}{\partial y}\right)^2+\sigma {B_0}^2u^2 \tag{3}$$

$$\frac{\partial C}{\partial t}+u\frac{\partial C}{\partial x}+v\frac{\partial C}{\partial y}=D\frac{\partial^2 C}{\partial y^2}-\gamma\left(C-C_\infty\right) \tag{4}$$

Subject to the following boundary conditions:

$$u = U_0 e^{\frac{x}{L}}, v = -V_0 e^{\frac{x}{L}}, T = T_w = T_\infty + T_0 e^{\frac{x}{2L}}, C = C_w = C_\infty + C_0 e^{\frac{x}{2L}} \quad at \quad y = 0$$
$$u \to 0, T \to T_\infty, C \to C_\infty \quad as \quad y \to \infty, \frac{\partial u}{\partial t} \neq 0, \frac{\partial T}{\partial t} \neq 0, \frac{\partial C}{\partial t} \neq 0 \tag{5}$$

where $u$ , $v$ are velocity component in the $x$ direction, velocity component in the $y$ direction, $C$, and $T$ are concentration of the fluid species and fluid temperature respectively. $L$ is the reference length, $B(x)$ is the magnetic field strength, $U_0$ is the reference velocity and $V_0$ is the permeability of the porous surface. The physical quantities $K$, $\rho$, $\nu$, $\sigma$, $D$, $k$, $C_p$, $Q_0$ and $\gamma$ are the permeability of the porous medium, density, fluid kinematics viscosity, electric conductivity of the fluid, coefficient of mass diffusivity, thermal conductivity of the fluid, specific heat, rate of specific internal heat generation or absorption and reaction rate coefficient respectively. $g$ is the gravitational acceleration, $\beta_T$ and $\beta_C$ are the thermal and mass expansion coefficients respectively. $q_r$ is the radiative heat flux in the $y$ direction. By using the Rosseland approximation, Ibrahim and Suneetha (2015), Amoo (2017), the radiative heat flux $q_r$ is given by

$$q_r = -\frac{4\sigma_0}{3\delta}\frac{\partial T^4}{\partial y} \tag{6}$$

where $\sigma_0$ and $\delta$ are the Stefan-Boltzmann and the mean absorption coefficient respectively. Assuming the temperature difference within the flow are sufficiently small such that $T^4$ may be expressed as a linear function of temperature, using Taylor series to expand $T^4$ about the free stream $T_\infty$ and neglecting higher order terms, this gives the approximation

$$T^4 \cong 4T_\infty^3 T - 3T_\infty^4 \tag{7}$$

The magnetic field $B(x)$ is assumed to be in the form $B(x) = B_0 e^{\frac{x}{2L}}$. (8)

Where $B_0$ is the constant magnetic field.

Introducing the stream function $u = \frac{\partial \psi}{\partial y}, v = -\frac{\partial \psi}{\partial x}$,

(9)

Continuity equation is satisfied when (9) is substituted in (1) and equations (2)-(4), give

$$\frac{\partial u}{\partial t} + \frac{\partial \psi}{\partial y}\frac{\partial^2 \psi}{\partial x \partial y} - \frac{\partial \psi}{\partial x}\frac{\partial^2 \psi}{\partial y^2} = -\frac{\sigma}{\rho} B_0 e^{\frac{x}{2L}}\left(\frac{\partial \psi}{\partial y}\right) + \nu\frac{\partial^3 \psi}{\partial y^3} + g\beta_T(T - T_\infty)\cos(\alpha) + g\beta_C(C - C_\infty)\cos(\alpha) \tag{10}$$

$$\frac{\partial T}{\partial t} + \frac{\partial \psi}{\partial y}\frac{\partial T}{\partial x} - \frac{\partial \psi}{\partial x}\frac{\partial T}{\partial y} = \left(\frac{k}{\rho C_p} + \frac{16\sigma_0 T_\infty^3}{3\rho C_p \delta}\right)\frac{\partial^2 T}{\partial y^2} + \frac{Q_0}{\rho C_p}(T - T_\infty) + \frac{\sigma}{\rho C_p} {B_0}^2 u^2 \tag{11}$$

$$\frac{\partial C}{\partial t} + \frac{\partial \psi}{\partial y}\frac{\partial C}{\partial x} - \frac{\partial \psi}{\partial x}\frac{\partial C}{\partial y} = D\frac{\partial^2 C}{\partial y^2} - \gamma(C - C_\infty) \tag{12}$$

The corresponding boundary conditions become:

$$\frac{\partial \psi}{\partial y} = U_0 e^{\frac{x}{L}}, \frac{\partial \psi}{\partial x} = V_0 e^{\frac{x}{L}}, T = T_w = T_\infty + T_0 e^{\frac{x}{2L}},$$

126
$$C = C_w = C_\infty + C_0 e^{\frac{x}{2L}} \quad at \quad y = 0 \qquad (13)$$
$$\frac{\partial \psi}{\partial y} \to 0, T \to T_\infty, C \to C_\infty \quad as \quad y \to \infty, \frac{\partial u}{\partial t} \neq 0, \frac{\partial T}{\partial t} \neq 0, \frac{\partial C}{\partial t} \neq 0$$

127 In order to transform the equations (11), (12) and (13) as well as the boundary conditions into an ordinary
128 differential equations, the following similarity transformations (variables) are introduced following Sajid and
129 Hayat (2008) and Amoo (2017).

130
$$\psi(x,y) = \sqrt{2\nu U_0 L} e^{\frac{x}{2L}} f(\eta), \eta = y\sqrt{\frac{U_0}{2\nu L}} e^{\frac{x}{2L}}, T = T_\infty + T_0 e^{\frac{x}{2L}} \theta(\eta), \qquad (14)$$
$$C = C_\infty + C_0 e^{\frac{x}{2L}} \phi(\eta)$$

131 Equations(11), (12)and(13) become

132
$$f''' - \frac{U}{2} f'' + ff'' - 2f'^2 - ((M + \frac{1}{B}) f' \left(f' + U\right) - Fs(f'^2) + G_r \theta \cos(\alpha) + G_c \phi \cos(\alpha) = 0 \qquad (15)$$

133
$$\left(1 + \frac{4}{3} R\right)\theta'' - P_r((\frac{\theta' U}{2} - f\theta') - 2U - f' - f'\theta + Q\theta + Ec(f)^2 + MEc(f')^2) = 0 \qquad (16)$$

134
$$\phi'' - Sc\frac{\phi U}{2} - Scf\phi' - 2USc\phi - Scf'\phi - Sc\lambda\phi = 0 \qquad (17)$$

135 The corresponding boundary conditions take the form:

136
$$f = f_w, f' = 1, \theta = 1, \phi = 1 \quad at \quad \eta = 0$$
$$f' = 0, \theta = 0, \phi = 0 \quad as \quad \eta \to \infty \qquad (18)$$

137 where $M = \frac{2\sigma L B_0}{\rho U_0} e^{\frac{x}{2L}}$ is the magnetic parameter, $Gc = \frac{2Lg\beta_T T_0}{U_0^2} e^{-\frac{3x}{2L}}$ is the thermal Grashof number,

138 $Gc = \frac{2Lg\beta_C C_0}{U_0^2} e^{-\frac{3x}{2L}}$ is the solutal Grashof number, $Pr = \frac{\rho\nu C_p}{k}$ is the Prandtl number, $R = \frac{4\sigma_0 T_\infty^3}{\delta k}$ is

139 the thermal radiation parameter, Ec= $\frac{u^2}{C_p(T_w - T_\infty)} = \frac{\mu}{\rho}$ is Eckert numbers, $F_s = \frac{2bx}{\sqrt{K}}$ is Forcheimmer

140 parameter, U is unsteady parameter, B is the porosity parameter, $Q = \frac{2LQ_0}{U_0 \rho C_p} e^{-\frac{x}{L}}$ is the heat generation

141 parameter, $Sc = \frac{\nu}{D}$ is the Schmidt number, $\lambda = \frac{2L\gamma}{U_0} e^{-\frac{x}{L}}$ is the chemical reaction parameter,

142 $f_w = V_0\sqrt{\frac{2L}{\nu U_0}} e^{-\frac{3x}{2L}}$ is the permeability of the plate.

143 The problem is a boundary value problem, applying a shooting technique (guessing the unknown values) to
144 change the conditions to initial value problem. In order to integrate equations (15), (16) and (17) as IVPs, the

values for $f''(0)$, $\theta'(0)$ and $\phi'(0)$ which were required for solution but no such values were given in the boundary. The suitable values for $f''(0)$, $\theta'(0)$ and $\phi'(0)$ were chosen and then integration was carried out. The researcher compared the calculated values for $f'(0)$, $\theta'(0)$ and $\phi(0)$ at $\eta = 3.5$ with the given boundary conditions $f'(3.5) = 0$ , $\theta'(3.5) = 0$ and $\phi(3.5) = 0$ Then adjusted the estimated values for $f''(0)$ , $\theta'(0)$ and $\phi'(0)$, to give a better approximation for the solution. The researcher performed the series of values for $f''(0)$, $\theta'(0)$ and $\phi'(0)$, and then applied a fourth-order Runge–Kutta method with shooting techniques with step-size $h = 0.01$. The value of $\eta_\infty$ is noticed to the iteration loop by $\eta_\infty = \eta_\infty + \Delta\eta$. The highest value of $\eta_\infty$ to each parameter is determined when the values of the unknown boundary conditions at $\eta = 0$ does not change after successful loop with error less than $10^{-5}$. The computations have been performed using a symbolic program and computational computer language Maple 18.

## RESULTS AND DISCUSSION

From the process of numerical computation, the skin-friction coefficient, the local Nusselt number and the local Sherwood number, which were respectively proportional to $f''(0)$, $\theta'(0)$ and $\phi'(0)$, at the plate were examined for different values of the parameters. The comparison of the present study with the skin friction of the existing works are presented in Table 1 for values of $\delta$ when Fs. = 0=U=0 = $\alpha$ =0 .

| **Values** | Present study | Devi et al (2015) | Kala, et al (2014 ). |
|---|---|---|---|
| M | $f''(0)$ | $f''(0)$ | $f''(0)$ |
| 0.0 | -0.000000 | -1.000480 | -1.000000 |
| 0.1 | -0.876889 | -0.872571 | -0.872083 |
| 0.5 | -0.646494 | -0.591683 | -0.591105 |

Table 1 shows numerical values of skin friction when compared with the existing literature and were in close agreement. The present study shows improvement over the previous studies. We validated our results by setting all newly introduced parameters U, Gr. Gc. $\lambda$ and $\alpha$ zero and were found to be in excellent agreement with Kala *et al* (2014), Devi et al (2015). The following parameter values are adopted for computation as default number: M=0.001, *Gr* =1, *Gc*= 0.1, $S_C$=0.35, $P_r$=0.72, R=0.5, Q=0.5, U=$f_w$=0.5, Fs=1 , B=0.5. All graphs were corresponded to the value except otherwise indicated on the graph.

**Table2:** Effect of M, $f_w$, $G_r$, $G_c$, $S_c$, $P_r$, and $R$ on $f''(0)$, $\theta'(0)$ and $\phi'(0)$ (P-Parameters)

| P | Values | $f''(0)$ | $-\theta'(0)$ | $-\phi'(0)$ | *P* | *Values* | $f''(0)$ | $-\theta'(0)$ | $-\phi'(0)$ |
|---|---|---|---|---|---|---|---|---|---|
| *M* | 0.001 | -3.8286 | -3.1423 | 0.8538 | Q | 0.5 | -3.0729 | -1.4290 | 1.7644 |
| | 2 | -4.2525 | -2.8213 | 0.8457 | | 0.8 | -3.1352 | -1.0542 | 1.7583 |
| | 3 | -4.4485 | -2.6984 | 0.8424 | | 1.0 | -3.1694 | -0.8495 | 1.7549 |
| | 4 | -4.6358 | -2.5925 | 0.8394 | | 1.5 | -3.2372 | -0.4433 | 1.7481 |
| $G_r$ | 0.01 | -4.2231 | -2.8825 | 0.8446 | Sc. | 0.35 | -3.0131 | -1.4348 | 1.2521 |

| | | | | | | | | | |
|---|---|---|---|---|---|---|---|---|---|
| | 3.1 | -3.6806 | -3.1316 | 0.8592 | | 0.62 | -3.0729 | -1.4290 | 1.7644 |
| | 3.8 | -3.5610 | -3.1829 | 0.8622 | | 1.50 | -3.1945 | -1.4219 | 3.1089 |
| | 5.0 | -3.3585 | -3.2669 | 0.8673 | | 2.00 | -3.2415 | -1.4203 | 3.7810 |
| *Gc.* | 1 | -3.9391 | -3.0503 | 0.8516 | $\lambda$ | 0.5 | -3.0729 | -1.4290 | 1.7644 |
| | 2 | -3.5671 | -3.7308 | 0.8754 | | 1.5 | -3.0944 | -1.4274 | 1.9670 |
| | 3 | -3.1748 | -4.3891 | 0.8981 | | 2.5 | -3.1125 | -1.4261 | -2.1469 |
| | 4 | -2.7806 | -4.9227 | 0.9187 | | 4.0 | -3.1353 | -1.4247 | -2.3873 |
| *fw.* | 1.00 | -3.0729 | -1.4290 | 1.7644 | *Fs.* | 1.00 | -3.0729 | -1.4290 | 1.7644 |
| | 2.00 | -3.4328 | -1.3669 | 2.1657 | | 2.00 | -3.1787 | -1.4260 | 1.7644 |
| | 3.00 | -3.8715 | -1.1770 | 2.6186 | | 3.00 | -3.2815 | -1.4229 | 1.7592 |
| | 4.00 | -4.3896 | -0.8989 | 3.1121 | | 5.00 | -3.4792 | -1.4167 | 1.7544 |
| *Pr* | 0.72 | -3.0729 | -1.4290 | 1.7644 | *Ec.* | 0.06 | -3.0021 | -1.7805 | 1.7690 |
| | 0.74 | -3.0639 | -1.4874 | 1.7653 | | 0.50 | -3.0729 | -3.1200 | -1.0971 |
| | 0.80 | -3.0368 | -1.6658 | 1.7677 | | 1.00 | -3.1952 | -0.5518 | 1.7534 |
| | 0.90 | -2.9912 | -1.9730 | 1.7717 | | 2.00 | -1.6782 | 0.4411 | 1.4193 |
| *R* | 0.50 | -3.0729 | -1.4290 | 1.7644 | *B* | 1 | 0.1632 | -1.3289 | 1.8792 |
| | 1.70 | -3.2246 | -0.4942 | 1.7496 | | 3 | 0.2545 | -1.3128 | 1.8828 |
| | 4.70 | -3.3048 | -0.0414 | 1.7409 | | 5 | 0.0528 | -1.3403 | 1.8750 |
| | 7.00 | -3.3235 | 0.0595 | 1.7387 | | 7 | -0.4037 | 1.3910 | 1.8578 |
| U | 0.10 | -1.1678 | 0.4411 | 1.4193 | $\alpha$ | 5 | -4.3419 | -0.8901 | 0.8275 |
| | 0.20 | -1.8531 | 0.2407 | 1.4614 | | 8 | -4.5375 | -0.8357 | 0.8179 |

| | | | | | | | | | |
|---|---|---|---|---|---|---|---|---|---|
| | 0.30 | -2.0223 | 0.0388 | 1.5024 | | 11 | -4.4686 | -0.8554 | 0.8214 |
| | 0.50 | -2.3445 | -0.3704 | 1.5815 | | 15 | -4.8272 | -0.7439 | 0.8021 |

Table 2 represents the numerical analysis of variation independent parameters (magnetic parameter, Darcy parameter, thermal Grashof number, Prandtl number, thermal radiation, Eckert, heat generation parameter, Schmidt number and chemical reaction and permeability of the plate surface) in explaining dependent parameters of Skin friction coefficient, Nusselt and Sherwood numbers at the surface. These further explain exponential analysis of velocity, temperature and concentration profiles thereby showing the effect of cross-diffusion on heat and mass transfer of unsteady MHD flow in porous media with dissipation and chemical reaction. All listed parameters are of physical and engineering interest. It was seen from the results that an increase in the values of $M$ , $Da$ , $fw$ , $Sc$ ,Pr. and $\lambda$ decrease the flow boundary layer while increase in $Gc$,$Gr$. $R$. $Q$. increased the flow boundary layer. The table depicts that an increase in the values of $M$, $Da$, $Q$, $Sc$. and $\lambda$ thicken the thermal boundary layer by reducing the rate at which heat diffuse out of the system as well as chemical reaction. The increase in $fw$ and Pr. reduce the thickness of the thermal boundary layer. It was also discovered that, increase in $fw$ , $Q$ , $Sc$ , $R$ and $\lambda$ cause thinning in the concentration boundary layer while $M$ , $Da$ and $Pr$. thicken the mass boundary layer.

## GRAPHICAL PRESENTATION OF THE STUDY

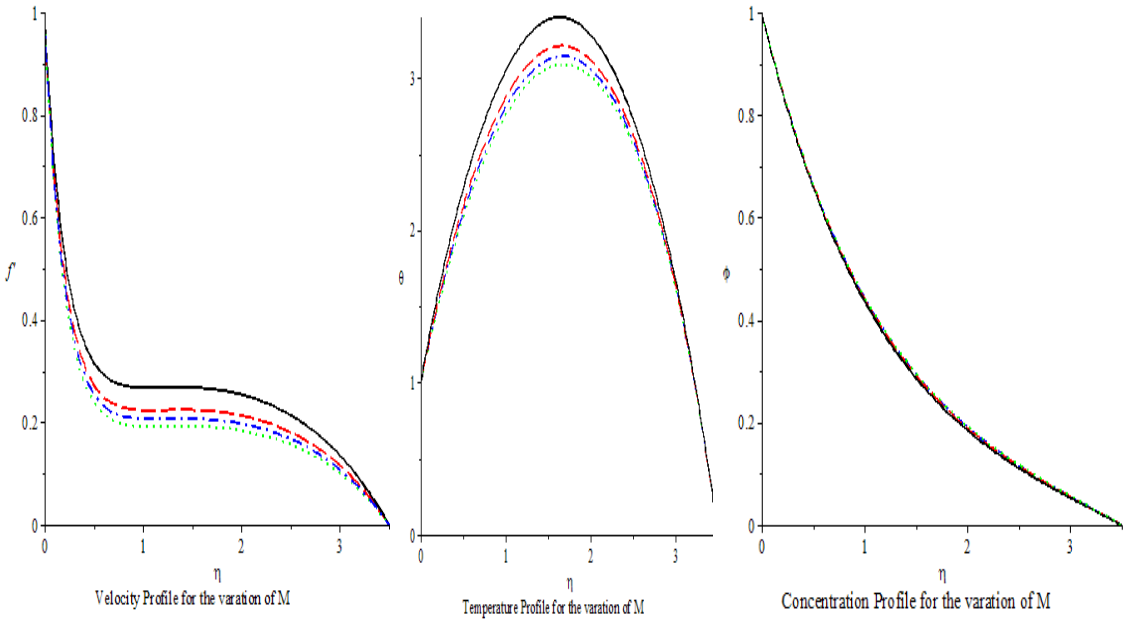


Figure 2

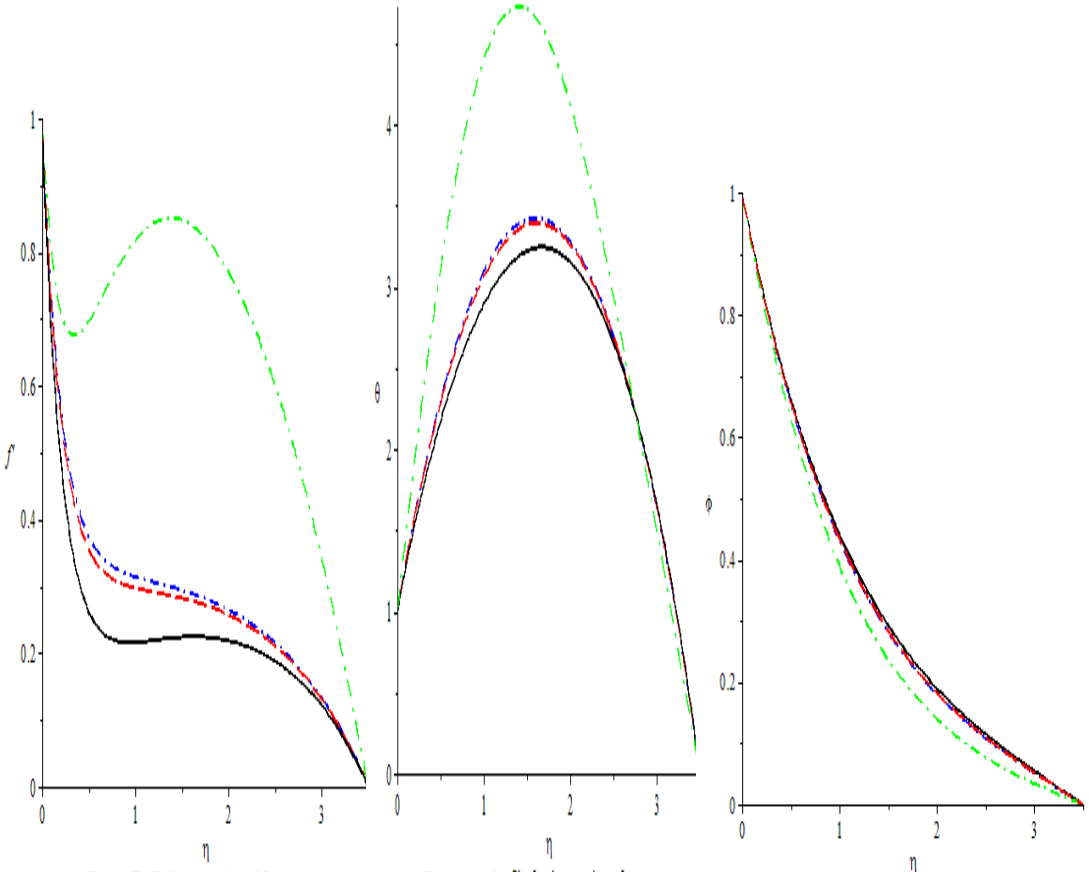


185

186 Figure 4

187

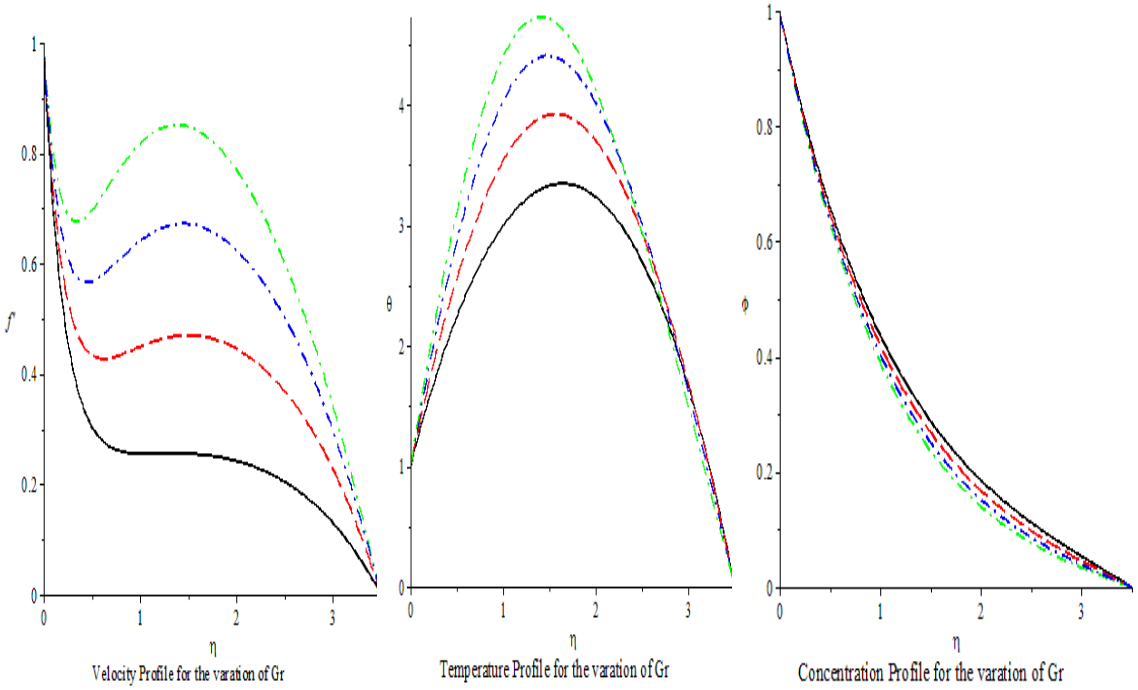


188

189 Figure 5

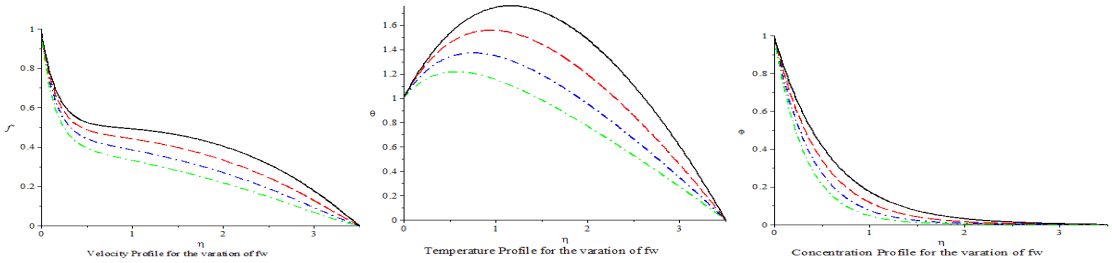


Figure 6

Figures 2, presents effects of magnetic field parameter on fluid flow or velocity, temperature and concentration profiles respectively. It was discovered in Figure 2 that increase in M slow down the rate of fluid flow thereby thinning the velocity boundary layer. It was discovered that temperature and chemical reaction parameter or concentration decreased. In this case, temperature and concentration at the boundary layer get thinner as magnetic field increased.

Figure 3 exhibits the effects of Gc on the exponential velocity, temperature and concentration respectively. The effect of solutal Grashof number on velocity distribution was illustrated in figure 3. It was noticed that increase in Gc led to increase in exponential velocity. The values of temperature increased with varied solutal Grashof number but decreased concentration when Solutal Grashof increased. These analyses are true of the figure 3 due to the fact that *Gc* usually increase when one talks about free or natural convection thereby increasing the velocity boundary layer flow.

Figure 5 exhibits the effects of varied thermal Grashof *Gr* parameter. It was discovered that velocity increased with increase in *Gr* but decrease in temperature and concentration profiles. The implication of this result suggested that slow rate of heat and free convective mass transfer was noticed. In this case, Gr slowed down the exponential temperature and concentration.

Figure 6 presented the effects of *fw* on the velocity, temperature and concentration profiles respectively. It was discovered that increase in *fw* parameter led to proportional decrease in rate of fluid flow, temperature or heat transfer as well as concentration profile or mass transfer. This parameter has more influence on velocity parameter because it is the parameter that explains the concept of porosity or permeability. The negative values explain the concept of suction while positive values of the parameter reveal the concept of injection. It was observed that suction decreased the exponential velocity, thereby indicating that suction stabilises the boundary layer development. Injection increases the velocity at the boundary layer thereby indicating that injection supports the flow to penetrate more into fluid.

In figure 6, it was discovered that temperature decreased as injection decreased, this suggests that injection does not induce cooling hence, fluid transfers to the surface. On the other hand, temperature decreases as suction increases, this means that suction leads to faster cooling of the plates. Figure 6 revealed the fact that concentration decreases as the suction increases and increases as the injection increases due to respective thinner and thickness in mass boundary layer.

## CONCLUSION

This study investigated unsteady MHD boundary layer flow, heat and mass transfer of an extended Darcy-Forcheimmer incompressible viscous fluid over porous stretching inclined surface in the presence of dissipation and chemical reaction. Skin friction, Nusselt and Sherwood numbers increased with increase in thermal Grashof parameter. Permeability at the plate decreased the skin friction but increased Nusselt and Sherwood numbers. The results showed that the velocity decreased with the increase in the value of radiation *R*. The fluid temperature decreased with the increase in thermal radiation while fluid temperature increased with an increase in Prandtl number. Darcy Forcheimmer parameter showed decrease in skin friction and Sherwood number, but increased Nusselt number. An increase in chemical reaction decreased skin friction and Nusselt number but increased Sherwood number. Eckert number increased the skin friction as well as Sherwood number but decreased the rate of heat in the flow. The study concluded that solutal Grashof, thermal Grashof, magnetic parameter, radiation parameter had significant effects on unsteady MHD

fluid flow in porous media stretching surface. This study is recommended for use in metallurgical applications and MHD power generation systems.

## REFERENCES


Abraham, J. P. and Sparrow, E. M. (2005) Friction Drag Resulting From the Simultaneous Imposed Motion of a Free stream and its Bounding Surface, *International Journal of Heat and Fluid Flow*, 26 (2), 289-295

Amoo, S. A (2017). Radiative Effects of Heat and Mass Transfer of MHD fluid flow in Porous Media. A paper presented at the African Institute for Mathematical Sciences, International Conference on Mathematics and its Applications, University of Buea, Republic of Cameroon, Central Africa, December, 12-14, 2017.

Amoo, S. A. and Babayo, A (2017) Numerical Analysis of MHD Heat and Mass Transfer Embedded in Darcy-forcheimmer Porous Medium with Dissipation and Chemical Reaction. Departmental Seminar Paper, Federal University Wukari, Wukari, Nigeria.

Amoo, S. A., Babayo, A and Amoo, A. O. (2017) Nonlinear MHD Boundary layer Flow Embedded in Darcy-forcheimmer Porous Medium with Dissipation and Chemical Reaction. In Lagos State University's Faculty of Science 5th Annual Conference, Ojo, Lagos between 10th and 14th October, 2017.

Baag, S. Mishra, S. R. Hoque, M. M., Anika, N. N (2018) Magnetohydrodynamics Boundary Layer Flow Over an Exponentially Stretching Sheet Past a Porous Medium with Uniform Heat Source, *Journal of Nanofluids, 7(3), 570-576*

Baag, S. Mishra, S. R. Nayak, B. and Acharya, M. R. (2017) Effect of radiation on MHD free convective flow over a stretching sheet in the presence of heat source / sink, *Defect and Diffusion Forum, 378, 1-15.*

Bhattacharyya, K (2011). Effects of radiation and heat source/sink on unsteady MHD boundary layer flow and heat transfer over a shrinking sheet with suction/injection, Front. Chem. Sci. Eng. 5, 376–384.

Bhukta, D, Dash, G.C, Mishra, S. R. and Baag, S. (2017) Dissipation effect on MHD mixed convective flow over a stretching sheet through porous medium with non-uniform heat source/sink, *Ain Shams Engineering Journal, 8, 353-361.*

Cortell, R. (2005). Flow and heat transfer of a fluid through a porous medium over a stretching surface with internal heat generation/ absorption and suction/blowing, Fluid Dynamics. Res. 37, 231–245.

Cortell, R. (2006). Effects of viscous dissipation and work done by deformation on the MHD flow and heat transfer of a viscoelastic fluid over a stretching sheet, Phys. Lett. A 357, 298–305.

Dash, G. C., Tripathy, R. S. Rashidi, M. M. and Mishra, S. R. (2016) Numerical approach to boundary layer stagnation-point flow past a stretching/shrinking sheet, *Journal of Molecular Liquids, 221, 860-866.*

Etwire,C.J. and Seini, Y,I. (2014) Radiative MHD flow over a vertical plate with convective boundary condition. In American Journal of Applied Mathematics 2(6): 214-220

Ibrahim, S. M. and Sunnetha, K. (2015). Effect of heat generation and thermal radiation on MHD flow near a stagnation point on a linear stretching sheet in porous medium and presence of variable thermal

conductivity and mass transfer. Journal of Computational and Applied Research in Mechanical Engineering 4(2), 133-144.

Kala, B. S. , Singh, M., and Kumar, A. (2014). Steady MHD free convective flow and heat transfer over nonlinearly stretching sheet embedded in an extended Darcyforcheimmer porous medium with viscous dissipation. Journal of Global Research in mathematical Achives, 2(4); 1-14.

Kaviany, M (1999), principles of Heat transfer in porous media. 2nd edition.. springer-verlas.

Khan, S. K. (2006). Boundary layer viscoelastic fluid flow over an exponentially stretching sheet, Int. J. Appl. Mech. Eng. 11, 321–335.

Kumar, D. S. (2013). *Heat and Mass Transfer*, S. K. Kataria and Sons, Punjab New Delhi, India.

Lakshmi, M.P, Reddy, N.B and Poornima, T (2012) MHD boundary layer flow of heat and mass transfer over a moving vertical plate in a porous medium with suction and viscous dissipation. International Journal of Engineering Research and Applications, ISSN: 2248-9622 2(5), 149-159.

Mishra, S.R. and Bhatti, M. M. (2017**)** Simultaneous effects of Chemical reaction and Ohmic heating with heat and mass transfer over a stretching surface: A numerical study, *Chinese Journal of Chemical Engineering, 25 (9), 1137-1142.*

Sajid, M. and Hayat,T (2008). Influence of thermal radiation on the boundary layer flow due to an exponentially stretching sheet, Int. Commun. Heat Mass Transfer 35, 347-356.

Sanjayanand, F. and Khan, S. K. (2006). On heat and mass transfer in a viscoelastic boundary layer flow over an exponentially stretching sheet, Int. J. Therm. Sci. 45, 819-828.

Sharma, P. K. (2004). Unsteady effect on MHD free convective and mass transfer flow through porous medium with constant suction and constant heat transfer past a semi-infinite vertical porous plate. Journal of Computational Materials and Science, 40, 186-192

Sparrow, E. M. and Abraham, J. P. (2005) Universal Solutions for the Streamwise Variation of the Temperature of a Moving Sheet in the Presence of a Moving Fluid. *International Journal of Heat and Mass Transfer*, 48, 3047-3056.

Thumma, T. and Mishra, S. R. (2018) Effect of viscous dissipation and Joule heating on Magnetohydrodynamics Jeffery nanofluid flow with and without multi-slip boundary conditions, *Journal of Nanofluids, 7(3), 516-526.*